Spin Physics Experiments at NICA-SPD with polarized proton and deuteron beams.

O. M. Kouznetsov[a]*, I. A. Savin[a]†

On behalf of the Letter of Intent (LoI) drafting committee

[a] *Joint Institute for Nuclear Research*

Joliot-Curie 6 141980 Dubna Moscow region Russia

30 October 2014

Abstract

We propose to perform measurements of asymmetries of the DY pair's production in collisions of non-polarized, longitudinally and transversally polarized protons and deuterons which provide an access to all leading twist collinear and TMD PDFs of quarks and anti-quarks in nucleons. The measurements of asymmetries in production of J/Ψ and direct photons will be performed simultaneously with DY using dedicated triggers. The set of these measurements will supply complete information for tests of the quark-parton model of nucleons at the QCD twist-two level with minimal systematic errors.

1 Introduction

This conference proceedings based on the Letter of Intent (LoI) [1] related to the studies of the nucleon structure on the NICA facility. The beginning of the nucleon structure story refers to the early 50-ties of the 20th century when in the famous Hofstadter's experiments at SLAC the proton electromagnetic form factor was measured determining thus the proton radius of $\langle r_p \rangle = (0.74\pm0.24) \cdot 10^{-13}$cm. It means that the proton is not an elementary particle but the object with an internal structure. Later on, again at SLAC, the point-like ***constituents*** have been discovered in the proton and called ***partons***. After some time, in 1970-ties, partons were identified with ***quarks*** suggested early by Gell-Mann as structureless constituents of all hadrons. Three families of quarks, each containing two quarks and anti-quarks, are now the basic elements of the Standard Model (SM) of elementary particle structure. All six quarks are discovered.

The naive quark-parton model (***QPM***) of nucleons has been born. According to this model, the protons (neutron) consist of three spin-1/2 ***valence quarks***: two (one) of the ***u***-type and one (two) of the ***d***-type with a charge of (+2/3) e and (-1/3) e, respectively, where e is the absolute value of the electron charge. Quarks interact between themselves by ***gluon*** exchange. Gluons are also the nucleon constituents. Gluons can produce a ***sea*** of any type (***flavor***) quark-anti-quark pairs. Partons share between themselves fractions, x, of the total nucleon momentum. Parton Distribution Functions (***PDFs***) are universal characteristics of the internal nucleon structure.

Now the quark-parton structure of nucleons and respectively the quark-parton model of nucleons are becoming more and more complicated. In Quantum Chromo Dynamics (QCD), PDFs depend not only on x, but also on Q^2, four-momentum transfer (see below). Partons can

---

*e-mail: Oleg.Kouznetsov@cern.ch

†e-mail: Igor.Savin@cern.ch

have an internal momentum, k, with possible transverse component, k_T. A number of PDFs depends on the order of the QCD approximations. Measurements of the collinear (integrated over k_T) and Transverse Momentum Dependent (TMD) PDFs, the most of which are not well measured or not discovered yet, are proposed in this LoI. **Main ideas of this document have been discussed at the specialized International Workshops [2].**

2 Basic (twist-2) PDFs of the nucleon.

There are three collinear PDFs characterizing the nucleon structure at the leading QCD order (twist-2). These PDFs are: the distribution of the parton Number in non-polarized (U) nucleon (**Density**), $f_1(x, Q^2)$; the distribution of longitudinal polarization of quarks in longitudinally polarized (L) nucleon (**Helicity**), $g_1(x, Q^2) \equiv g_{1L}(x, Q^2)$; and the distribution of transverse polarization of quarks in transversely polarized (T) nucleon (**Transversity**), $h_1(x, Q^2)$. They are shown as diagonal terms in Fig.1 with the nucleon polarization (U, L, T) along the vertical direction and the quark polarization along the horizontal direction. The PDF $h_1(x, Q^2)$ is poorly studied. It is a chiral-odd function which can be measured in combination with another chiral-odd function.

If one takes into account the possible transverse momentum of quarks, k_T, there will be five additional Transverse Momentum Dependent (TMD) PDFs which are functions of three variables: x, k_T, Q^2. These TMD PDFs are: correlation between the transverse polarization of nucleon (transverse spin) and the transverse momentum of non-polarized quarks (**Sivers**), $f_{1T}^\perp$; correlation between the transverse spin and the longitudinal quark polarization (**Worm-gear-T**), $g_{1T}^\perp$; distribution of the quark transverse momentum in the non-polarized nucleon (**Boer-Mulders**), $h_1^\perp$; correlation between the longitudinal polarization of the nucleon (longitudinal spin) and the transverse momentum of quarks (**Worm-gear-L**), $h_{1L}^\perp$; distribution of the transverse momentum of quarks in the transversely polarized nucleon (**Pretzelosity**), $h_{1T}^\perp$. All new PDFs, except $f_{1T}^\perp$, are chiral-odd. The Sivers and Boer-Mulders PDFs are T-odd ones. At the sub-leading twist (twist-3), there are still 16 TMD PDFs containing the information on the nucleon structure. They have no definite physics interpretation yet.

Figure 1: The twist-2 PDFs characterizing the nucleon structure. The nucleon polarization (U, L, T) is shown along the vertical direction and the quark polarization is shown along the horizontal direction

The new TMD PDFs are chiral odd and can be measured only in the Semi-inclusive DIS (SIDIS) or Drell-Yan (DY) processes. So far data have been obtained for the polarized nucleon only from SIDIS by the HERMES and COMPASS collaborations. Polarized TMD PDFs from the DY processes in πp interactions are to be measured at COMPASS-II [3]. There is a real

opportunity and challenge to study TMD PDFs at NICA in polarized *pp*- and *pd*- collisions. In SIDIS, the chiral TMD PDFs can be obtained studying the azimuthal modulations of hadrons which are sensitive to convolution of PDF with the corresponding FF. The PDFs f_1 and g_1 are measured rather well. The h_1 has been measured recently but is still poorly investigated. All TMD PDFs are currently underthe study. The status of these PDFs measurement is summarized in [4] and updated in [5]. The collinear and TMD PDFs are necessary for complete description of the nucleon structure at the level of twist-2 approximation. **Its precision measurement at NICA can be the main subject of the NICA SPD spin program.**

3 Physics motivations.

3.1 The Drell-Yan mechanismas a tool for the nucleon structure studies.

The Drell-Yan process of the di-lepton production in high-energy hadron-hadron collisions (Fig. 2) is playing an important role in the hadron structure studies.
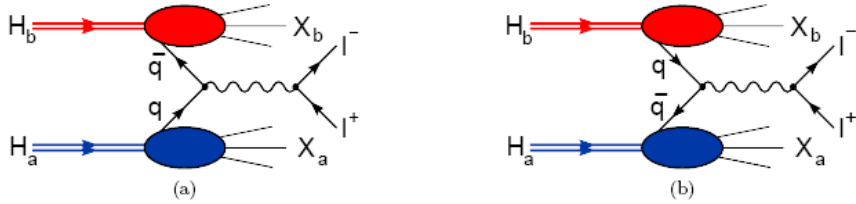

Figure 2: The parton model diagrams of the di-lepton production in collisions of hadrons $H_a(P_a, S_a)$ with hadrons $H_b(P_b, S_b)$. The constituent quark (anti-quark) of the hadron H_a annihilates with constituent anti-quark (quark) of the hadron H_b producing the virtual photon which decays into a pair of leptons $l^\pm$ ($e^\pm$ or $\mu^\pm$). The hadron spectator systems X_a and X_b are usually not detected. Both diagrams have to be taken into account.

The kinematics of the Drell-Yan process can be most conveniently considered (Fig.3) in the Collins-Soper (CS) reference frame [6],[7],[8],[9]. The transition from the hadrons-center-of-mass frame (CM-frame) to the CS-frame is described in [6]. The CS-frame includes three intersecting planes. The first one is the *Lepton plane* containing vectors of the lepton momenta, *l, l'* (in the lepton rest frame), and the unit vector in the z-direction, where tgα =q_T/q, q_T ($q = l+l'$, $q \equiv Q$) is the transverse momentum (momentum) of the virtual photon in the CM-frame. The second plane, the *Hadron or Collins-Soper* plane, contains the momentum of colliding hadrons, P_a, P_b, and vector is the unit vector in the direction of the photon transverse momentum, and the third plane – *Polarization plane* – contains the polarization vector $S \equiv \mathbf{S}_T$ ($\mathbf{S}_{aT}$, $\mathbf{S}_{bT}$) and the unit vector. The ϕ is the azimuthal angle between the *Lepton* and *Hadron* planes; ϕ_S(i.e. ϕ_{Sa} or ϕ_{Sb})is the angle between the *Lepton* and *Polarization* planes and θ is the polar angle of $\mathbf{l}$ in the CS-frame.
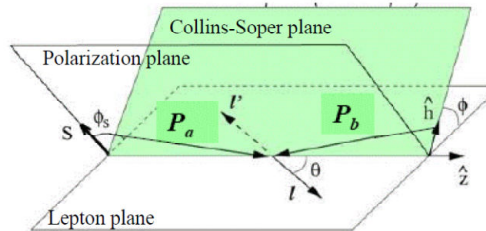

Figure 3: Kinematics of the Drell-Yan process in the Collins-Soper reference frame.

The most complete theoretical analysis of the DY process, for cases when both hadrons H_a and H_b, in our case protons or deuterons, are polarized or non-polarized, was performed in [18].

The differential cross section of the DY pair's production in the quark-parton model via PDFs [6] is rewritten (Fig.4) in LoI in the more convenient variables with a change of notations of the azimuthal angle polarization vectors as in Fig.3.

$$\frac{d\sigma}{dx_a dx_b d^2q_T d\Omega} = \frac{\alpha^2}{4Q^2} \times$$

$$\Big\{ \big((1+\cos^2\theta) F_{UU}^1 + \sin^2\theta \cos 2\phi F_{UU}^{\cos 2\phi} \big) + S_{aL} \sin^2\theta \sin 2\phi F_{LU}^{\sin 2\phi} + S_{bL} \sin^2\theta \sin 2\phi F_{UL}^{\sin 2\phi}$$

$$+ |\vec{S}_{aT}| \Big[\sin(\phi - \phi_{S_a})(1+\cos^2\theta) F_{TU}^{\sin(\phi-\phi_{S_a})} + \sin^2\theta \big(\sin(3\phi - \phi_{S_a}) F_{TU}^{\sin(3\phi-\phi_{S_a})} + \sin(\phi + \phi_{S_a}) F_{TU}^{\sin(\phi+\phi_{S_a})} \big) \Big]$$

$$+ |\vec{S}_{bT}| \Big[\sin(\phi - \phi_{S_b})(1+\cos^2\theta) F_{UT}^{\sin(\phi-\phi_{S_b})} + \sin^2\theta \big(\sin(3\phi - \phi_{S_b}) F_{UT}^{\sin(3\phi-\phi_{S_b})} + \sin(\phi + \phi_{S_b}) F_{UT}^{\sin(\phi+\phi_{S_b})} \big) \Big]$$

$$+ S_{aL} S_{bL} \Big[(1+\cos^2\theta) F_{LL}^1 + \sin^2\theta \cos 2\phi F_{LL}^{\cos 2\phi} \Big] \qquad\qquad (2.1.2)$$

$$+ S_{aL} |\vec{S}_{bT}| \Big[\cos(\phi - \phi_{S_b})(1+\cos^2\theta) F_{LT}^{\cos(\phi-\phi_{S_b})} + \sin^2\theta \big(\cos(3\phi - \phi_{S_b}) F_{LT}^{\cos(3\phi-\phi_{S_b})} + \cos(\phi + \phi_{S_b}) F_{LT}^{\cos(\phi+\phi_{S_b})} \big) \Big]$$

$$+ |\vec{S}_{aT}| S_{bL} \Big[\cos(\phi - \phi_{S_a})(1+\cos^2\theta) F_{TL}^{\cos(\phi-\phi_{S_a})} + \sin^2\theta \big(\cos(3\phi - \phi_{S_a}) F_{TL}^{\cos(3\phi-\phi_{S_a})} + \cos(\phi + \phi_{S_a}) F_{TL}^{\cos(\phi+\phi_{S_a})} \big) \Big]$$

$$+ |\vec{S}_{aT}| |\vec{S}_{bT}| \Big[(1+\cos^2\theta) \big(\cos(2\phi - \phi_{S_a} - \phi_{S_b}) F_{TT}^{\cos(2\phi-\phi_{S_a}-\phi_{S_b})} + \cos(\phi_{S_b} - \phi_{S_a}) F_{TT}^{\cos(\phi_{S_b}-\phi_{S_a})} \big) \Big]$$

$$+ |\vec{S}_{aT}| |\vec{S}_{bT}| \Big[\sin^2\theta \big(\cos(\phi_{S_a} + \phi_{S_b}) F_{TT}^{\cos(\phi_{S_a}+\phi_{S_b})} + \cos(4\phi - \phi_{S_a} - \phi_{S_b}) F_{TT}^{\cos(4\phi-\phi_{S_a}-\phi_{S_b})} \big) \Big]$$

$$+ |\vec{S}_{aT}| |\vec{S}_{bT}| \Big[\sin^2\theta \big(\cos(2\phi - \phi_{S_a} + \phi_{S_b}) F_{TT}^{\cos(2\phi-\phi_{S_a}+\phi_{S_b})} + \cos(2\phi + \phi_{S_a} - \phi_{S_b}) F_{TT}^{\cos(2\phi+\phi_{S_a}-\phi_{S_b})} \big) \Big] \Big\}$$

Figure 4: The cross section of the DY pair's production in the QPM via LO PDFs, where F_{jk}^i are the Structure Functions (SFs) connected to the corresponding PDFs. The SFs F_{jk}^i give more detailed information on the nucleon structure than usual structure functions depending on two variables x_{Bj} and Q^2.

The azimuthal distribution of DY pair's produced in non-polarized hadron collisions, A_{UU}, and azimuthal asymmetries of the cross sections in polarized hadron collisions, A_{jk}, are shown in Fig.5:

A number of conclusions can be drawn comparing some asymmetries to be measured. The measured asymmetries A_{LU} and A_{UL} and assume that during these measurements the beam polarizations are equal, i.e. $|S_{aL}| = |S_{bL}|$, and hadrons a,b are identical. Then one can intuitively expect that the integrated over x_a and x_b asymmetries $A_{LU} = A_{UL}$. Similarly, comparing the asymmetries A_{TU} and A_{UT} or A_{TL} and A_{LT} one can expect that $A_{TU}^1 = A_{UT}^1$ and $A_{TL}^1 = g_{LT}^1$. **The tests of these expectations will be a good check of the parton model approximations.**

The large number of independent SFs to be determined from the polarized DY processes at NICA (24 for identical hadrons in the initial state) is sufficient to map out all eight leading twist TMD PDFs for quarks and anti-quarks. This fact indicates the high potential of the polarized DY process for studying new PDFs. This process has also a certain advantage over SIDIS [10],[11] which also capable of mapping out the leading twist TMD PDFs but requires knowledge of fragmentation functions.

The transverse single-spin asymmetries depending on the Structure Functions or are of the particular interests. The both SFs contain the Sivers PDF which was predicted to have the opposite sign in DY as compared to SIDIS [12],[13],[14]. **As the sign reversal is at the core of our present understanding of transverse single spin asymmetries in hard scattering processes, the experimental check of this prediction is of the utmost importance.** The expected sign reversal of T-odd TMDs can also be investigated through the structure functions in which the Boer-Mulders PDF enters [15].[16],[17].

It is very important to measure those new TMD PDFs which are still not measured or measured with large uncertainties. These are Worm-gear-T, L and Pretzelosity

4

$$A_{UU} \equiv \frac{\sigma^{00}}{\sigma_{int}^{00}} = \frac{1}{2\pi}(1 + D\cos 2\phi A_{UU}^{\cos 2\phi})$$

$$A_{LU} \equiv \frac{\sigma^{\rightarrow 0} - \sigma^{\leftarrow 0}}{\sigma_{int}^{\rightarrow 0} + \sigma_{int}^{\leftarrow 0}} = \frac{|S_{aL}|}{2\pi} D\sin 2\phi A_{LU}^{\sin 2\phi}$$

$$A_{UL} \equiv \frac{\sigma^{0\rightarrow} - \sigma^{0\leftarrow}}{\sigma_{int}^{0\rightarrow} + \sigma_{int}^{0\leftarrow}} = \frac{|S_{bL}|}{2\pi} D\sin 2\phi A_{UL}^{\sin 2\phi}$$

$$A_{TU} \equiv \frac{\sigma^{\uparrow 0} - \sigma^{\downarrow 0}}{\sigma_{int}^{\uparrow 0} + \sigma_{int}^{\downarrow 0}} = \frac{|\vec{S}_{aT}|}{2\pi} \left[A_{TU}^{\sin(\phi-\phi_{S_a})} \sin(\phi-\phi_{S_a}) + D\left(A_{TU}^{\sin(3\phi-\phi_{S_a})} \sin(3\phi-\phi_{S_a}) + A_{TU}^{\sin(\phi+\phi_{S_a})} \sin(\phi+\phi_{S_a}) \right) \right]$$

$$A_{UT} \equiv \frac{\sigma^{0\uparrow} - \sigma^{0\downarrow}}{\sigma_{int}^{0\uparrow} + \sigma_{int}^{0\downarrow}} = \frac{|\vec{S}_{bT}|}{2\pi} \left[A_{UT}^{\sin(\phi-\phi_{S_b})} \sin(\phi-\phi_{S_b}) + D\left(A_{UT}^{\sin(3\phi-\phi_{S_b})} \sin(3\phi-\phi_{S_b}) + A_{UT}^{\sin(\phi+\phi_{S_b})} \sin(\phi+\phi_{S_b}) \right) \right]$$

$$A_{LL} \equiv \frac{\sigma^{\rightarrow\rightarrow} + \sigma^{\leftarrow\leftarrow} - \sigma^{\rightarrow\leftarrow} - \sigma^{\leftarrow\rightarrow}}{\sigma_{int}^{\rightarrow\rightarrow} + \sigma_{int}^{\leftarrow\leftarrow} + \sigma_{int}^{\rightarrow\leftarrow} + \sigma_{int}^{\leftarrow\rightarrow}} = \frac{|S_{aL}S_{bL}|}{2\pi} \left(A_{LL}^1 + D A_{LL}^{\cos 2\phi} \cos 2\phi \right)$$

$$A_{TL} \equiv \frac{\sigma^{\uparrow\rightarrow} + \sigma^{\downarrow\leftarrow} - \sigma^{\downarrow\rightarrow} - \sigma^{\uparrow\leftarrow}}{\sigma_{int}^{\uparrow\rightarrow} + \sigma_{int}^{\downarrow\leftarrow} + \sigma_{int}^{\downarrow\rightarrow} + \sigma_{int}^{\uparrow\leftarrow}} = \frac{|\vec{S}_{aT}| S_{bL}}{2\pi} \left[A_{TL}^{\cos(\phi-\phi_{S_a})} \cos(\phi-\phi_{S_a}) + D\left(\begin{array}{c} A_{TL}^{\cos(3\phi-\phi_{S_a})} \cos(3\phi-\phi_{S_a}) \\ + A_{TL}^{\cos(\phi+\phi_{S_a})} \cos(\phi+\phi_{S_a}) \end{array} \right) \right]$$

$$A_{LT} \equiv \frac{\sigma^{\rightarrow\uparrow} + \sigma^{\leftarrow\downarrow} - \sigma^{\rightarrow\downarrow} - \sigma^{\leftarrow\uparrow}}{\sigma_{int}^{\rightarrow\uparrow} + \sigma_{int}^{\leftarrow\downarrow} + \sigma_{int}^{\rightarrow\downarrow} + \sigma_{int}^{\leftarrow\uparrow}} = \frac{S_{aL} |\vec{S}_{bT}|}{2\pi} \left[A_{LT}^{\cos(\phi-\phi_{S_b})} \cos(\phi-\phi_{S_b}) + D\left(\begin{array}{c} A_{LT}^{\cos(3\phi-\phi_{S_b})} \cos(3\phi-\phi_{S_b}) \\ + A_{LT}^{\cos(\phi+\phi_{S_b})} \cos(\phi+\phi_{S_b}) \end{array} \right) \right]$$

$$A_{TT} \equiv \frac{\sigma^{\uparrow\uparrow} + \sigma^{\downarrow\downarrow} - \sigma^{\uparrow\downarrow} - \sigma^{\downarrow\uparrow}}{\sigma_{int}^{\uparrow\uparrow} + \sigma_{int}^{\downarrow\downarrow} + \sigma_{int}^{\uparrow\downarrow} + \sigma_{int}^{\downarrow\uparrow}} = \frac{|\vec{S}_{aT}| \| \vec{S}_{bT}|}{2\pi} \Big[A_{TT}^{\cos(2\phi-\phi_{S_a}-\phi_{S_b})} \cos(2\phi-\phi_{S_a}-\phi_{S_b}) + A_{TT}^{\cos(\phi_{S_a}-\phi_{S_b})} \cos(\phi_{S_a}-\phi_{S_b})$$

$$+ D\Big(A_{TT}^{\cos(\phi_{S_b}+\phi_{S_a})} \cos(\phi_{S_a}+\phi_{S_b}) + A_{TT}^{\cos(4\phi-\phi_{S_a}-\phi_{S_b})} \cos(4\phi-\phi_{S_a}-\phi_{S_b})$$

$$+ A_{TT}^{\cos(2\phi-\phi_{S_a}+\phi_{S_b})} \cos(2\phi-\phi_{S_a}+\phi_{S_b}) + A_{TT}^{\cos(2\phi+\phi_{S_a}-\phi_{S_b})} \cos(2\phi+\phi_{S_a}-\phi_{S_b}) \Big) \Big] \qquad (2.1.10)$$

Figure 5: Eight asymmetries to be measured: ALU, AUL, ATU , AUT, ALL, ATL, ALT, ATT.

PDFs. The last one would give new information (at least within some models) on the possible role of constituent's orbital momenta in the resolution of the nucleon spin crisis.

3.2 Direct photons.

Direct photon productions in the non-polarized and polarized *pp(pd)* reactions provide information on the gluon distributions in nucleons. There are two main hard processes where direct photons can be produced: gluon Compton scattering, $g + q \rightarrow \gamma + X$, and quark-anti-quark annihilation, $q + \bar{q} \rightarrow \gamma + X$. As it has been pointed out in [19], "the direct photon production in non polarized *pp* collisions can provide a clear test of short-distance dynamics as predicted by the perturbative QCD, because the photon originates in the hard scattering sub-process and does not fragment. This immediately means that Collins effect is not present. The process is very sensitive to the non polarized gluon structure function, since it is dominated by quark-gluon Compton subprocess in a large photon transverse momentum range". The total cross section of the direct photon production in the *pp*-collision at $\sqrt{s}$=24 GeV via the Compton scattering (according to PYTHIA 6.4) is equal to 1100 nb, while the cross section of the annihilation is about 200 nb. So, the gluon Compton scattering is the main mechanism of the direct photon production. The extraction of the polarized gluon distribution (Sivers gluon function) can be done [19] from measurement of the transverse single spin asymmetry A_N defined as follows: $A_N = \frac{\sigma\uparrow - \sigma\downarrow}{\sigma\uparrow + \sigma\downarrow}$ where $\sigma\uparrow$ and $\sigma\downarrow$ are the cross sections of the direct photon production for the opposite transverse polarizations of one of the colliding protons. In [21] it has been pointed out that the asymmetry A_N at large positive x_F is dominated by quark-gluon correlations

while at large negative x_F [22] it is dominated by pure gluon-gluon correlations. The further development of the corresponding formalism can be found in [23], [24].

The first attempt to measure A_N at $\sqrt{s}$=19.4 GeV was performed in the fixed target experiment E704 at Fermilab [20] in the kinematic range -0.15< x_F <0.15 and 2.5< p_T <3.1 GeV/c. Results are consistent with zero within large statistical and systematic uncertainties.

The single spin asymmetries in the direct photon production will be measured also by PHENIX [25] and STAR [26] at RHIC. Production of direct photons at large transverse momentum with longitudinally polarized proton beams is a very promising method to measure gluon polarization Δg [27].

3.3 Spin-dependent effects in elastic pp, dp, dd scattering and spin-dependent reactions in heavy ion collisions.

There are several spin-dependent effects in elastic and quasi-elastic scattering reactions which could be further studied at NICA.

- The charge-exchange $dp \rightarrow (pp)_S n$ reaction.

- Forward elastic pd-scattering and $pN \rightarrow pN$ amplitudes.

- Backward elastic pd-scattering and the hard deuteron breakup $pd \rightarrow (pp)_S n$.

- Investigation of the birefringence phenomenon at NICA facility.

- Inclusive particle polarizations in heavy-ion collisions.
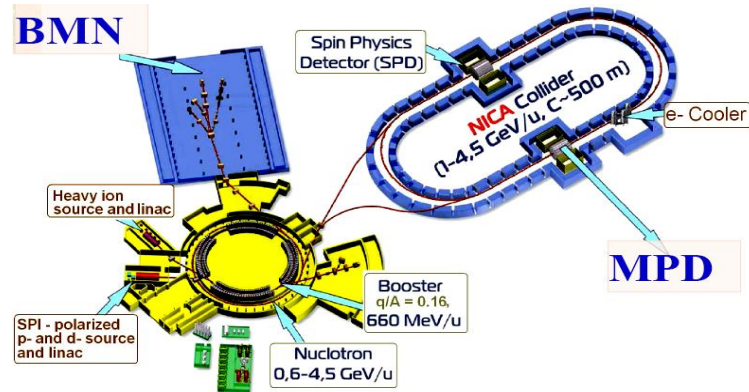
4 The NUCLOTRON-NICA complex.

Figure 6: Layout of the NUCLOTRON-NICA complex.

The NICA complex at JINR has been approved in 2008 assuming two phases of the construction. The first phase, is being realized now, includes construction of facilities for heavy ion physics program [28] while the second phase should include facilities for the program of spin physics studies with accelerated polarized protons and deuterons.

The main elements of NICA complex are shown in Fig.6. They include: the heavy ion source and source of polarized ions (proton and deuteron), SPI, with corresponding Linacs, existing superconducting accelerator Nuclotron upgraded to Nuclotron M, new superconducting Booster
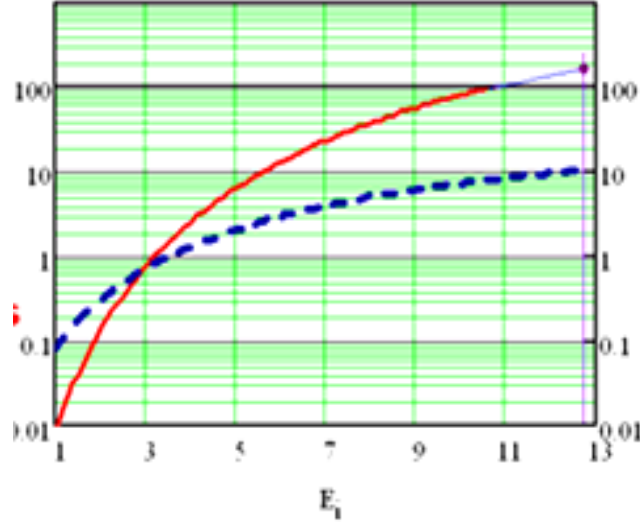
Figure 7: NICA pp luminosity in units 10^{30} (left scale, solid line) and number of particle per bunch in units $10^{11} cm^{-2} s^{-1}$ (right scale, dotted line) vs. the proton kinetic energy.

synchrotron , new collider NICA with two detectors – MPD (Multi-Purpose Detector) for heavy ion interaction studies and SPD (Spin Physics Detector), as well as experimental hall for fixed target experiments with beams extracted from Nuclotron M.

The research program requires definite characteristics of beams polarized and non-polarized: $pp, pd, dd, pp^\uparrow, pd^\uparrow, p^\uparrow p^\uparrow, p^\uparrow d^\uparrow, d^\uparrow d^\uparrow$. Beam polarizations both at MPD and SPD: longitudinal and transversal. Absolute values of polarizations during the data taking should be 90-50%. The life time of the beam polarization should be long enough. Measurements of Single Spin and Double Spin asymmetries in DY require running in different beam polarization modes: UU, LU, UL,TU, UT,LL ,LT and TL (spin flipping for every bunch or group of bunches should be considered).

Beam energies: $p^\uparrow p^\uparrow \sqrt{s_{pp}} = 12 \div \geq 27$ GeV (5 ÷ ≥12.6 GeV kinetic energy), $d^\uparrow d^\uparrow \sqrt{s_{NN}} = 4 \div \geq 13.8$ GeV (2 ÷ ≥5.9 GeV/u ion kinetic energy). Asymmetric beam energies should be considered also.

Beam luminosities: in the pp mode (Fig.7): $L_{average} \geq 1 \cdot 10^{32}$ cm^{-2}s^{-1} (at $\sqrt{s_{pp}} = 27$ GeV) and in the dd mode: $L_{average} \geq 1 \cdot 10^{30}$ cm^{-2}s^{-1} (at $\sqrt{s_{NN}} = 14$ GeV).

For estimations of the expected statistics of events, we assume that total efficiency of the NICA complex will be $\geq 80\%$.

4.1 Requirements to the spin physics detector (SPD).

Requirements for SPD are motivated by physics and, first of all, by a topology of events and particles to be detected. SPD should operate at the highest possible luminosity. So, all the SPD sub-detectors should have high rate capabilities and preserve high efficiency during a long time. It is useful to remember that in the energy range of NICA the total cross section of pp interactions is almost constant, about 40 mb, and expected event rates at the luminosity 10^{32}cm^{-2}s^{-1} will be $4 \cdot 10^6$ per second. The average particle multiplicities estimated with PYTHIA at $\sqrt{s} = 24$ GeV are the following: charged particles –13.5, neutral particles – 22.5. The clean DY events can be detected in region of invariant mass 4 – 9 GeV.

4.2 Possible layout of SPD.

Preliminary considerations of the event topologies required SPD to be equipped with the following sub-detectors covering $\sim 4\pi$ angular region around the beam intersection point: vertex detectors, tracking detectors, electromagnetic calorimeters, hadron and muon detectors. Some of them must be in the magnetic field for which there are two options: either toroid or solenoid type.
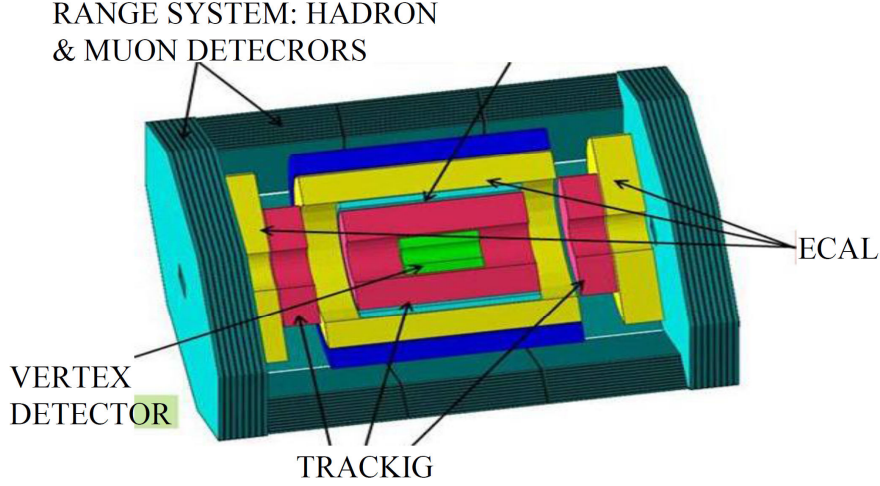

Figure 8: Possible layout of SPD with the solenoid magnet.

Possible SPD layout with the solenoid magnet is shown in Fig.8. The magnet part of SPD, usually called "barrel", contains inside a vertex detector, tracking detectors and electromagnetic calorimeters (ECAL). Outside of the barrel one needs to have muon and hadron detectors. The end-cap part of SPD could contain a tracking, ECAL, and range systems. The solenoid SPD version could have almost 100% azimuthal acceptance, which is important, for example, for detection of some exclusive reactions. Disadvantage of the solenoid option is a presence of the magnetic field in the beam pipe region. This field can disturb beam particle trajectories and their polarization. Screening of this field should be studied.

The dimension of the SPD volume is still an open question. It should be optimized basing on compromise between the precisions and costs. The "almost 4π geometry" requested by DY and direct photons can be realized in the solenoid version of SPD if it has overall length and diameter of about 6 m.

5 Proposed measurements with SPD.

We propose to perform measurements of asymmetries of the DY pair's production in collisions of polarized protons and deuterons which provide an access to all collinear and TMD PDFs of quarks and anti-quarks in nucleons. The measurements of asymmetries in production of J/Ψ and direct photons will be performed simultaneously with DY using dedicated triggers. The set of these measurements will supply complete information for tests of the quark-parton model of nucleons at the twist-two level with minimal systematic errors.

5.1 Estimations of the DY production rates and precisions of asymmetry measurements.

Estimation of the DY pair's production rate at SPD was performed using the expression [29] for the differential and total cross sections of the pp interactions. The Table 5.1 shows values

of the cross-sections and expected statistics for DY events per 7000 hours of data taking and 100% acceptance of SPD at two energies.

Lower cut on M_{l+l-}, GeV	2.0	3.0	3.5	4.0
$\sqrt{s}$=24 GeV ($L = 1.0 \cdot 10^{32}$ cm^{-2} s^{-1})				
σ_{DY} total, nb	1.15	0.20	0.12	0.06
events per 7000h, 10^3	1800	313	179	92
$\sqrt{s}$=26 GeV ($L = 1.2 \cdot 10^{32}$ cm^{-2} s^{-1})				
σ_{DY} total, nb	1.30	0.24	0.14	0.07
events per 7000h, 10^3	2490	460	269	142

Table 5.1 Estimations of the DY production rates and precisions of asymmetry measurements.

To estimate the precision of asymmetry measurements, the set of original software packages for MC simulations, including generators for Sivers, Boer-Mulders and Transversity PDFs, were developed [30]. With these packages a sample of 100K DY events was generated in the region of $Q^2 >11$ GeV^2 for comparison with expected asymmetries.

The estimated q_T- weighted integrated asymmetry Sivers as a function of $x_p - x_{p\uparrow}$ is shown in the Fig.9.
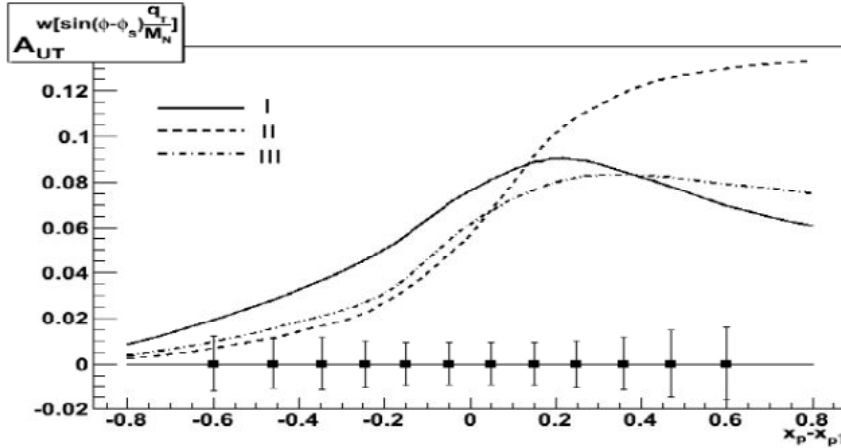

Figure 9: Estimated Sivers asymmetry at $\sqrt{s}$=26 GeV with Q^2= 15 GeV^2. Numbers I, II, III denote differrent fits. Points with the expected statistical errors correspond to 100K of generated events

As one can see from this Fig.9, the expected integrated Sivers asymmetries depend on the PDF parameterization and vary in the whole region of $x_p - x_{p\uparrow}$ from about 1 to 12%. Statistics of 100K is marginally enough to distinguish between the fits.

The estimated q_T- weighted integrated asymmetry Boer-Mulders as a function of $x_p - x_{p\uparrow}$ is shown in the Fig.10.

5.2 Estimations of the J/Ψ production rates and precisions of asymmetry measurements.

Statistics of the J/Ψ and DY events (with cut on M_{l-l+}= 4 GeV) expected to be recorded ("per year") in 7000 hours of data taking with 100% efficiency of SPD are given in Table 5.2.
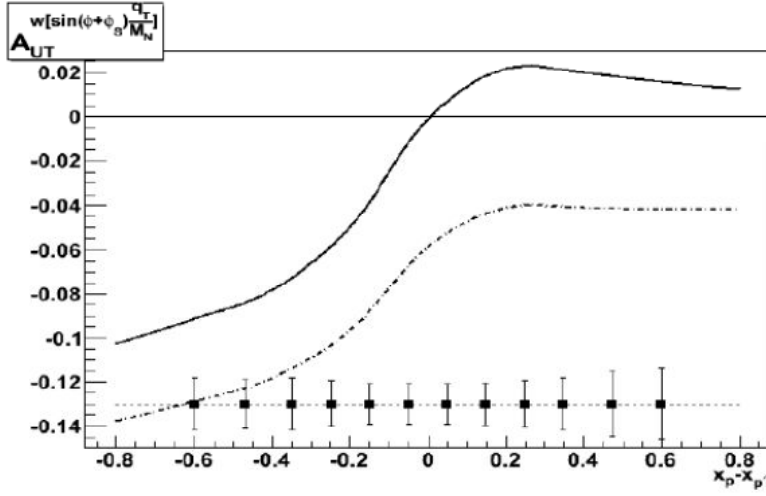
Figure 10: Estimations of Boer-Mulders asymmetry at $\sqrt{s}$ =26 GeV and Q^2= 15 GeV^2. The solid and dotted curves correspond to the first and second versions of the evolution model, respectively. Points with bars show the expected statistical errors obtained with 100K of events

$\sqrt{s}$, GeV	24	26	$\sqrt{s}$, GeV	24	26
$\sigma_{J/\Psi} \cdot B_{e+e-}$, nb	12	16	σ_{DY} , nb	0.06	0.07
Events "per year"	$18 \cdot 10^6$	$23 \cdot 10^6$	Events "per year"	$92 \cdot 10^3$	$142 \cdot 10^3$

Table 5.2: Comparison of the J/Ψ and DY statistics

5.3   Estimations of direct photon production rates.

Estimation of the direct photon production rates based on PYTHIA6 Monte-Carlo simulation is presented in Table5.3 for two values of colliding proton energies. Event rates are given for all and for leading processes of direct photon production considered in PYTHIA assuming 7000 hours of operation at maximal luminosity. Statistical accuracies of A_N and A_{LL} measurements at NICA have been estimated assuming the beam polarizations (both transversal and longitudinal) equal to $P = \pm 0.8$ and overall detector efficiency (acceptance, efficiency of event reconstruction and selection criteria) of about 50%. Under such assumption, after 7000 hours of data taking the A_N and A_{LL} could be measured with statistical accuracy of ~0.11% and ~0.18%, respectively, in each of 18 x_F bins (-0.9< x_F < 0.9). Large statistics of events provide opportunities to measure the asymmetries as a function of x_F and p_T. To minimize systematic uncertainties, precision of luminosity and beam polarization should be under control, as well as accuracy of π^0, η and other background rejection.

Table 5.3: Estimated rates of the direct photon production.

$\sqrt{s}$=24 GeV $L = 1.0 \times 10^{32},\ cm^{-1}s^{-1}$	σ_{tot}, nbarn	$\sigma_{P_T>4\ GeV/c}$, nbarn	Events/year, 10^6	Events/year, 10^6 ($P_T > 4\ GeV/c$)
All processes	1290	42	3260	105
$qg \to q\gamma$	1080	33	2730	84
$q\bar{q} \to g\gamma$	210	9	530	21
$\sqrt{s}$=26 GeV $L = 1.2 \times 10^{32},\ cm^{-1}s^{-1}$	σ_{tot}, nbarn	$\sigma_{P_T>4\ GeV/c}$, nbarn	Events/year, 10^6	Events/year, 10^6 ($P_T > 4\ GeV/c$)
All processes	1440	48	4340	144
$qg \to q\gamma$	1220	38	3680	116
$q\bar{q} \to g\gamma$	240	10	660	28

6 Possible data taking scenario.

At the first step of the project it is reasonable to start measurements with non-polarized protons (pp) and with non-polarized deuterons (dd), (pd). These data would provide a cross checks of our results with very precise world data on f_1 PDFs. At the same time new data on the Boer-Mulders PDF will be obtained.

At the second step the measurements should be performed with longitudinally polarized protons and deuterons in pp, pd and dd collisions with the beam polarizations UL, LU, LL to obtain asymmetries A_{LU}, A_{UL} and A_{LL} in each case. These data will be cross checked by existing data on g_1 PDF and provide new information on the Worm-gear-L PDF in proton and neutron (u & d quarks).

At the third step (the most important) measurements should be performed with transverse beam polarization in pp, pd and dd collisions (UT, TU and TT) to obtain asymmetries A_{UT}, A_{TU} and A_{TT} in each case. These data will be cross checked by existing data on Transversity PDF and provide new information on the Sivers, Worm-gear-T and Pretzelosity PDFs in proton and neutron (u & d quarks).

Finally, at the fourth step (the most difficult) measurements should be performed with pp, pd and dd beams when one beam polarized longitudinally while other – transversally in order to measure asymmetries A_{LT} and A_{TL} in each case. These data will provide new information and cross checks of our results on Transversity, Worm-gear-L, Pretzelosity and Worm-gear-T PDFs.

References

[1] Letter of Intent presented at the meeting of the JINR Program Advisory Committee (PAC) for Particle Physics on 25-26 June 2014; arXiv:1408.3959[hep-ex]

[2] http://nica.jinr.ru/files/SPIN_program/NICA-SPD2013/index.html,
http://nica.jinr.ru/files/SPIN_program/SPIN-Praha-2013/index.html,
http://theor.jinr.ru/∼spin/2013/

[3] COMPASS-II Proposal, CERN-SPSC-2010-014, SPSC-P-340, May 2010.

[4] C. Marchand, in Proceedings of the XX International Workshop on Deep-Inelastic Scattering and Related Subjects, Bonn, Germany, 26-30 March 2012, and references therein.

[5] B. Parsamyan, Proceedings of DIS 2013 International Conf., PoS DIS 2013, 231(2013), [arXiv:1307.0183 [hep-ex], and references therein.

[6] J.C. Collins and D.E. Soper, Phys. Rev. **D16** (1977) 2219.

[7] J.C. Collins, D.E. Soper, and G. Sterman, Nucl. Phys. **B250** (1985)199.

[8] X. Ji, J.P. Ma, and F. Yuan, Phys. Rev. **D71**, 034005 (2005), [arXiv:hep-ph/0404183].

[9] J.C. Collins and A. Metz, Phys. Rev. Lett. **93**(2004) 252001,

[10] P.J. Mulders and R.D. Tangerman, Nucl. Phys. **B461**(1996) 197, [Erratum-ibid. **B484**(1997)] 538, [arXiv:hep-ph/9510301].

[11] A. Bacchetta, M. Diehl, K. Goeke, A. Metz, P. Mulders and M. Schlegel, [arXiv:hep-ph/0408249].

[12] S.J. Brodsky, D.S. Hwang, and I. Schmidt, Phys. Lett. **B530**(2002) 99,[arXiv:hep-ph/0201296].

[13] J.C. Collins, Phys. Lett. **B536** (2002) 43, [arXiv:hep-ph/0204004].

[14] S.J. Brodsky, D.S. Hwang, and I. Schmidt, Nucl. Phys. **B642**(2002) 344; [arXiv:hep-ph/0206259].

[15] A. Sissakian, O. Shevchenko, A. Nagaytsev, and O. Ivanov, arXiv:0807.2480 [hep-ph].

[16] A. Sissakian, O. Shevchenko, A. Nagaytsev and O. Ivanov, Phys. Rev. **D72**(2005) 054027), [arXiv:hep-ph/0505214].

[17] A. Sissakian, et al., Eur. Phys. J. **C46** (2006)147, [arXiv:hep-ph/0512095].

[18] S. Arnold, A. Metz and M. Schlegel, Phys. Rev. **D79** (2009) 034005, [arXiv:hep-ph/0809.2262].

[19] I. Shmidt, J. Soffer and J.J. Yang, Phys. Lett. **B612** (2005) 258-262.

[20] D. L. Adams et al., Phys. Lett. **B345**(1995) 569-575.

[21] J. Qui and G. Sterman, Phys. Rev. Lett. **67** (1991) 2264; Nucl. Phys. B 378 (1992) 52.

[22] J. Xiandong, Phys. Lett. **B289**(1992) 137.

[23] N. Hammon et al., Phys. G: Nucl. Part. Phys. **24** (1998) 991-1001.

[24] L. Gamberg and Z. Kang, Phys. Lett. **B718**(2012) 181.

[25] S. Campbell: "Prompt photon measurements with PHENIX's MPC-EX detector", talk at Nuclear Dynamics, 2013, https://www.phenix.bnl.gov/phenix/WWW/talk/archive/2013/ndww13/t2103.pdf

[26] Len K. Eun, http://meetings.aps.org/link/BAPS.2011.DNP.HC.3.

[27] Cheng HY, Lai SN. Phys. Rev. **D4** (1990) 91-102.

[28] V.D. Kekelidze, A.D. Kovalenko, R. Lednicky, V.A. Matveev, I.N. Meshkov, A.S. Sorin,G.V. Trubnikov, Status of NICA project at JINR, PoS(Baldin ISHEPP XXI) 085, p. 1-9, SISSA, Italy.

[29] I.V.Andreev, QCD in hard processus at high energy. M. 1981

[30] A.Sissakian, O.Shevchenko, A.Nagaytsev, and O.Ivanov, Phys.Part.Nucl. 41 (2010) 64-100.